Materials Science & Engineering C 105 (2019) 110113

Contents lists available at ScienceDirect

Materials Science & Engineering C

journal homepage: www.elsevier.com/locate/msec

A fluorescence Nano-biosensors immobilization on Iron (MNPs) and gold (AuNPs) nanoparticles for detection of *Shigella spp*

Narges Elahi[a,d], Mehdi Kamali[a,*], Mohammad Hadi Baghersad[b], Bahram Amini[c,*]

[a] Nano biotechnology Research Center, Baqiyatallah University of Medical Sciences, Tehran, Iran
[b] Applied Biotechnology Research Center, Baqiyatallah University of Medical Sciences, Tehran, Iran
[c] Department of Biochemistry, Zanjan University of Medical Sciences, Zanjan, Iran
[d] Department of Medical Nanotechnology, Schcool of Advance Medical Scinces and Technologies, Shiraz University of Medical Scinces, Shiraz, Iran.

ARTICLE INFO

Keywords:
Fluorescence biosensor
Shigella
Spa gene
MNPs
AuNPs

ABSTRACT

The highly sensitive and specificity detection are very important in diagnosis of foodborne pathogens and prevention of spread diseases. Therefore, in the present study, a highly sensitive fluorescence Nano-biosensors was designed for detection of *Shigella* species. For achieved this purpose, DNA probes and gold nanoparticles (AuNPs) were designed and synthesized, respectively. Then, two DNA probes as signal reporter were immobilized on surface of AuNPs. On the other hand, Iron nanoparticles (MNPs) were synthesized and modified with SMCC (Sulfosuccinimidyl 4-Nmaleimidomethyl cyclohexane-1- carboxylate). The 3th DNA probe was immobilized on surface of MNPs for separation of target DNA. The MNP-DNA probe and DNA probe-AuNP-fluorescence DNA probe were added to target DNA. The MNP- DNA probe-target DNA-DNA probe-AuNP-fluorescence DNA probe complex was isolated by a magnet. The fluorescence DNA probe was released on surface of AuNPs and the fluorescence intensity was read by fluorescence spectrophotometry. Sensitivity and specificity of designed Nano-biosensor was determined. The results showed that the fluorescence intensity was increased with increasing of target DNA concentration. Linear related between target DNA and fluorescence intensity was observed in 2.3×10^2 up to 2.3×10^7 CFU mL^{-1}. The linear equation and regression were $Y = 1.8\ X + 23.4$ and R^2 0.9953. Limit of detection (LOD) were determined 90 CFUmL^{-1}. The specificity of Nano-biosensor in present of other bacteria was confirmed.

1. Introduction

According to the World Health Organization (WHO), foodborne diseases are very important in public health and increased in the both developed and developing countries. *Salmonella*, *Shigella*, and diarrhea genic *E. coli* are prevalently cause bacterial diarrhea in children under the age of five. Among these pathogens, the *Shigella* has very important in inflammatory diarrhea and dysentery. Consequently, it introduces a serious challenge for public health authorities worldwide [1]. Ultra-sensitive, rapid, and reliable analysis as well as the detection of food-borne pathogens at an early stage is an indispensable component of strategies for the prevention of the outbreak of foodborne diseases, which are crucial threats to human health [2,3].

Accessible bacteria detection can be divided into two categories: conventional and modern methods [4,5]. Microbiological plating, microscopic visualization, biochemical tests, nucleic-acid-based methods, and immunologic method are the conventional analytical methods for *Shigella* detection [4–6]. PCR [7], multiplex PCR [8–10], multiplex real-time PCR [11–14], and Loop-mediated isothermal amplification (LAMP) [15] are the number of the nucleic-acid-based techniques that there are employed for *Shigella* detection. High cost, need for special tools, the need to preparing samples and expensive are limited of use this methods [16–18]. Therefore, rapid, sensitive, and specific methods for bacteria detection are necessary.

Recently, biosensor-based methods, as the modern generation of detection, have progressed to a great extent [19,20]. Some of applied biosensors in the microbial analysis of foodborne pathogens are the optical-based, SPR-based, piezoelectric-based, immune-based, and electrochemical-based-sensors. The superiority of biosensors has numerous reasons, but the main reasons are that they enable fast or real-time detection and they provide the specific, sensitive, on-site diagnosis of analyses with minimal samples, while granting portability and multi-pathogen detection for both field and laboratory analyses [4,6]. The applications of biomaterials in biosensors are providing scopes for new

* Corresponding authors.
E-mail addresses: mehkamali@yahoo.co.uk (M. Kamali), bamini50@yahoo.com (B. Amini).

https://doi.org/10.1016/j.msec.2019.110113
Received 10 April 2019; Received in revised form 19 August 2019; Accepted 21 August 2019
Available online 22 August 2019
0928-4931/

signal transduction technology [21,22]. Gold nanoparticles (AuNPs) and magnetic nanoparticles (MNPs) are the two main metallic particles in designed biosensor. MNPs are providing various facile and cost-effective methods for synthesis and allow the easy separation of reacted target molecules from unreacted molecules [22,25–31]. On the other hand, the AuNPs could bond with thiols, disulfides, and amines groups. These properties are used in designing different types of biosensors that the using in colorimetry assay, fluorescence assay, luminesce assay, SPR, and fluorescence bio-barcode assay [22–24]. Florescence-based sensors are very important in detection of macromolecules such as tumor markers, nucleic acids, proteins, carbohydrates and antibodies. Fluorescence labeling can be built based on metal nanoparticles, quantum dots, nanotubes, etc. [4,21,26–33]. The accessibility of various synthesis methods along with the feasibility of post synthetic modifications proposes a wide range of functionality to fluorescent nanomaterials [4,21,34]. Bio-recognition probes of the biosensor are responsible for the specific detection of the analyses. Commonly employed bio-probes for pathogen detection are nucleic acids, antibodies, whole phages, phage-display peptides (PDPs), and most recently phage's receptor binding proteins (RBPs). DNA-based probes are applying simple, stable, versatile, rapid, and cost-effective detection with high selectivity and sensitivity [16].

In the present study, novel fluorescent Nano-biosensors was designed and immobilized on AuNPs and MNPs modified with SMCC for detection of *Shigella spp* for the first time. First, AuNP and MNP nanoparticles were synthesized by the citrate reduction method and the polyol technique in an autoclave (121 °C), respectively. Then, two DNA probes and a florescence DNA probe were designed for detection of *Shigella* spp. A DNA probe was immobilized on surface MNPs with SMCC linker. Two DNA probes immobilized on AuNPs as signal reporter and connected macromolecules. Under optimum condition, DNA probe-AuNP-florescence DNA probe and MNP-DNA probe were added to target DNA to formed MNP-DNA probe-target DNA-DNA probe-AuNP-florescence DNA probe complex. The sandwich complex was isolated by a magnet and washed three times. The florescence DNA probe on surface of AuNPs was released by DTT (0.8 M) and florescence intensity was measured by florescence spectrophotometry. Finally, sensitive and specificity of designed Nano-biosensor were determined.

2. Materials and methods

2.1. Materials

Sodium citrate dehydrates, hydrogen tetro-chloroaurate (III) trihydrate, $FeCl_3{\cdot}6H_2O$, sodium hydroxide, sodium acetate, ethylenediamine, ethylene glycol, Dithiothreitol (DTT), ethyl acetate, NaCl, Luria broth (LB-broth) were prepared from Merck, Com, Germany. SMCC (Sulfosuccinimidyl 4-Nmaleimidomethyl cyclohexane-1- carboxylate) and SNHS (Sulfo-NHS acetate) were prepared from Thermo, Com, USA. All DNA probes were prepared from Bioneer, Com, Korea. *S. aureus* ATCC27217, *P. aeruginosa* ATCC27853, *Shigella boydii* ATCC9207, *Shigella felxneri* ATCC12022, *Shigella sonnei* ATCC9290, *Shigella dysantri* ATCC12022, *V. cholera* ATCC51394 as the positive and negative controls were prepared from Pasteur Institute, Tehran, Iran.

2.2. Apparatus

Autoclave (Tomy XS-700, Japan) was used as a reactor for MNPs synthesis. DLS (Malvern, USA) was used for characterization of size and potential of nanoparticles. Functional groups and bonds within MNPs were determined using Fourier Transformed Infrared (FTIR; Perkin RXI FT-IR Spectrometer, USA). Magnetic properties of MNPs were characterized by vibrating sample magnetometer (VSM; Meghnatis Kavir, IRAN). Thermocycler PCR (Bio Rad, USA) was used for generate target DNA. Gel electrophoresis (Bio Rad, USA) was used for conformed the PCR product. DNA purification kit (Pure Link Genomic DNA Mini Kit) was used for purification of genomic DNA of bacteria. Nanodrop 2000c UV–Vis Array spectrophotometer (Laboratory Industrial and Research System, Teif Sanj Pishro Pajohesh, Iran) was used to measure the concentration of DNA. TEM (Transmission Electron Microscope) (ZEISS EM10C, Carl Zeiss AG, Oberkochen, Germany) was used for characterization of the nanoparticles. Fluorescence Spectrophotometer (Perkin Elmer LS 55, USA) was used for measuring the fluorescence intensity.

2.3. Bacteria species

Four species of *Shigella spp*, including: *S. flexneri*, *S. boydii*, *S. sonnei* and *S. dysenteriae* were used as positive control. The *E. coli*, *V. cholera*, *S. aureus* and *P. aeruginosa* were used as negative controls for diagnostic specificity of Nano-biosensor. For target DNA extraction, the bacterial strains were grown on LB-broth overnight. Subsequently, 5 mL of culture media contain bacteria was centrifuged and isolated at 1500 rpm for 10 min. The DNA was extracted by the DNA Purification Kit. The extracted DNA concentration was researched using a UV–Vis spectrophotometry at 260 nm wavelength.

2.4. Determination of microbial quantity

The pour-plate technique was applied in order to determine the microbial quantity. First, 1 mL of liquid sample was added to 9 mL of D.D.W. Serial dilution was conducted between 10^{-3} and 10^{-4} dilution factors to obtain countable bacteria colonies on agar plates. Then, the samples were completely mixed and plate on proper media. The total plate counts were determined by plating out 1 mL of diluted samples from 10^{-2} and 10^{-4} with sterile pipette into sterile Petri discs. Nutrient agar was sterilized in an autoclave at 121 °C for 15 min. Then, cool agar was poured into the plate and allowed to set. Then, the plates were incubated in the incubator at 37 °C between 24 and 48 h. At last, the developed colonies on the agar plates were counted.

2.5. Designing biosensors

The *Spa* sequence was used for designing of DNA probes. Briefly, the *Spa* gene sequence was isolated of Genbank, NCBI and designed DNA probes by DNASIS and Oligo software. The DNA probes and fluorescence DNA probe sequence were showed in following. The thiol groups on the DNA probes were conjugated on surface of AuNPs and MNPs. The Fluorescence $probe_2$ was labeled with Texas Red 613 (TEX $_{613}$ λ_{ex} 596 nm and λ_{em} 613 nm) as signal reporter.

DNA $probe_1$ (AuNPs): 5′AAGCTGGTTCGAAAGTATTthiol-3′.

Fluorescence DNA $probe_2$ (AuNPs): 5'TEX_{613}TTATTCGTAGCTAAA AAAAAAAthiol3′.

DNA $probe_3$ (MNPs): 5'thiolTTAAGAGTGGGGTTTGATG3′.

2.6. Synthesis of AuNPs

According protocols Amini et al. and Shi et al., the citrate reduction method was used for synthesis of AuNPs [21,26,35,37–40]. All the glassware was washed with aqua regia (HCl and HNO_3 3:1). Briefly, 100 mL of $HAuCl_4$ (1 mM) was boiled with stirring at 700 rpm. Sodium citrate solution (38.5 mM, 5 mL) was added dropwise to reaction mixture. The color solution was changed from yellow to purple within seconds. After about 2 min was changed to deep red that indicating the formation of AuNPs. The reaction was performed for 20 min at 100 °C with 700 rpm. Subsequently, the heater was turned off to the cooled AuNPs at room temperature with 700 rpm. Colloidal AuNPs were stored at 4 °C. The absorbance maximum of AuNPs was determined by UV–Vis Array Spectrophotometer (Laboratory Industrial and Research System, Teif Sanj Pishro Pajohesh Com, Iran). Structure, potential and size of AuNPs was measured using Transmission Electron Microscopy (TEM) and Dynamic light Scattering (DLS).

2.7. Synthesis of MNPs

Amino-functionalized magnetic nanoparticles were prepared in single step process, using polyol technique in an autoclave (121 °C) without insert gas as described by *Songvorawit* et al. [41,45]. Briefly, 2 g of $FeCl_3{\cdot}6H_2O$ was added into 40 mL ethylene glycol and mixed until the solution was changed to clear yellow. Then, 6 g of CH_3COONa, 2.50% W/V of NaOH and 20 mL of ethylene diamine (source of amino group) were added to reaction mixture and stirred for 30 min. The mixed solution was further heated in an autoclave at 121 °C, 105 KPa, for 6 h. After the reaction was completed, amino-MNPs were isolated by magnet filed and washed with distilled water and 95% ethanol several times to remove the solvent. The amino-MNPs were dried and stored in a dry bottle. The characterization of particles was defined by DLS, FTIR, and VSM techniques.

2.8. Functionalization of nanoparticles

In the present study, the DNA probes for detection of *Shigella spp* were conjugated on surface of MNPs and AuNPs. The DNA probes were formed disulfide band together, and then there were unable to interactions with nanoparticles. Therefore, DNA probes must be active before used.

2.8.1. AuNPs functionalization

In order to, firstly, DNA probe and Fluorescence DNA probe were added to 100 μL of 1.0 N dithiothreitol solution (1.0 N DTT: 0.01 M Sodium acetate (pH 5) 20 mL, 1.545 g DTT dissolve) at 25 °C for 15 min. After, braked disulfide band between DNA probes, the DTT was extracted of reaction mixture with added 200 μl ethyl acetate. After stirring for 2 min at 700 rpm, the upper layer was discarded. DNA probe concentrations were measured using Nano Drop UV–Vis spectrophotometry. The purified Fluorescence DNA probe (5 nmol) and DNA probe (0.05 nmol) were immediately added to 1 mL of the AuNPs synthesized previously. Fig. 1A showed the AuNPs functionalization and incubated in a dark place at room temperature for 14 h. In order to, stabilized AuNPs for long-time the salt (NaCl, 0.1 M up to 1 M) was serially added reaction mixture and storage at 25 °C [40–44]. The efficiency of conjugated DNA probes on surface of AuNPs was analyzed by Nano Drop and fluorescence spectrophotometry.

$$E.\ C = (C_T - C_S)/C_T \times 100$$

where, E.C: Percentage of conjugation of DNA probe, C_T: Primary concentration of the DNA probe, Cs: Concentration of the DNA probe at supernatant after released DNA probes on surface of AuNPs.

2.8.2. MNPs functionalization

For functionalized MNPs, 1 mg of MNPs was added to 1 mL coupling buffer (CB: NaCl 0.2 M, PBS buffer 0.1 M, pH 7.4) contain 300 μg of SMCC for 2–3 h. The MNP-SMCC was separated from supernatant and washed three times with CB. Then, the reduced DNA $probe_3$ (5 nmol) was added into 1 mL CB contain MNP-SMCC. The reaction was performed for 8–10 h; at 25 °C. Fig. 1B schematically showed the MNP-SMCC-DNA probe conjugation. The conjugated MNP-SMCC with DNA $probe_3$ was separated by a magnetic field and washed three times with CB. For inactive MNP-SMCC amin group, 35 mL of Sulfo-NHS acetate (10 mM) was added to MNP-SMCC-DNA $probe_3$ for 1–2 h at 25 °C. The blacked MNP-SMCC- DNA $probe_3$ was isolated by a magnetic field and washed three times with passivation buffer (Tris 0.2 M, pH 8.5). The MNP-SMCC- DNA $probe_3$ was suspended in storage buffer (PBS 100 mM, NaCl 0.2 M, pH 7.4).

2.9. Detection of target DNA

Diluted different concentration of target DNA were added to 0.5 mL micro tubes and incubated at 95 °C for 10 min in the PCR thermocycler to double strand DNA was converted to single strand DNA. 200 μL of assay buffer (PBS 100 mM, NaCl 0.15 M, SDS 0.1%, pH 7.4, 1 mg MNP-SMCC- DNA $probe_3$) was added to each micro tubes contain single strand DNA and incubated 48 °C for 45 min. The connected target DNA to MNP-SMCC-DNA $probe_3$ was isolated by magnetic field and washed three times with assay buffer. Then, 50 μL of Fluorescence DNA $probe_2$-AuNP-DNA $probe_1$ complex was added to each micro tube contain MNP-SMCC-DNA $probe_3$ (200 μL) and incubated at 48 °C for 1 h. After the formation of sandwich structure (MNP-SMCC-DNA $probe_3$-target DNA Fluorescence DNA $probe_2$-AuNP-DNA $probe_1$), the supernatant was removed using magnetic field (Fig. 1). The washing processes have been continued with 500 μl of the assay buffer five times until the whole amount of the unreacted solution components was perfectly removed. The sandwich complex was stored at 4 °C for final analysis.

2.10. Fluorescence assay

The fluorescence DNA $probe_2$ was labeled by 5′-TEX 613 as a fluorophore which its Excitation wavelength at 596 nm and Emission wavelength at 613 nm. Fluorescence intensity was measured by the PerkinElmer LS 55 fluorescence spectrometry. For the fluorescence intensity measurements, the fluorescence DNA $prob_2$ must be released on surface of AuNPs. So, the MNP-SMCC-DNA $probe_3$-target DNA-Fluorescence DNA $probe_2$-AuNP-DNA $probe_1$ sandwich was prepared in different concentration of extracted DNA of bacteria (CFU mL^{-1}). Then, the Fluorescence DNA $probe_2$ was released by the following steps. First, the MNP-SMCC-DNA $probe_3$-target DNA-Fluorescence DNA $probe_2$-AuNP- DNA $probe_1$ sandwich was resolved in 100 μL of DTT solution (0.8 M) and incubated at 50 °C for 15 min, with vortexed at 700 rpm. Then, the released fluorescence DNA $probe_2$ was separated of reaction mixture by magnetic field. The supernatant was contained fluorescence DNA $probe_2$ that the fluorescence intensity was determined by a fluorescence spectrometry (Fig. 1).

3. Results and discussion

3.1. Characterization of NPs

3.1.1. TEM and DLS

The size, shape and potential of synthesized AuNPs and MNPs were researched using of Transmission Electron Microscopy (TEM) and Dynamic light scattering (DLS). The results of before and after conjugation of DNA probes with AuNPs and MNPs showed in Fig. 2. The TEM images were indicated that the shape of AuNPs and MNPs were spherical and semi-spherical with dimension of 15 nm, charge of −32.2 mV and 23–28 nm, −25 mV, respectively (Fig. 2A, B, G and H). The size and potential of the AuNPs after conjugation was changed form 15 nm, −32.2 mV and 23–28 nm, −25 mV to 18 nm, −18 mV and 43 nm, −15 mV, respectively (Fig. 2C, D, E, F, J, K, L and Z).

3.1.2. VSM

The magnetic properties of the synthesized MNP-NH_2 were analyzed by the VSM technique at room temperature. Fig. 2X showed the magnetic properties. Synthesized nanoparticles have magnetization curves that were very close to complete super paramagnetic.

3.1.3. FTIR

$FeCl_3{\cdot}6H_2O$, as a precursor of magnetic particles and ethylene diamine as an amino group source, were utilized for the preparation of MNP-NH_2. These nanoparticles were modified to attach an amino group onto their surface, which was ready for the conjugation of any biomolecules. Functional groups and the chemical bonds of MNPs, such as the existence of the amino group on the particle surface were determined by FTIR spectroscopy. Fig. 2W, curve A, curve B and curve C showed the FTIR spectra of amino-MNPs, amino-MNPs-DNA $probe_3$ and fluorescence DNA $probe_2$-AuNP-DNA $probe_1$ over the range of

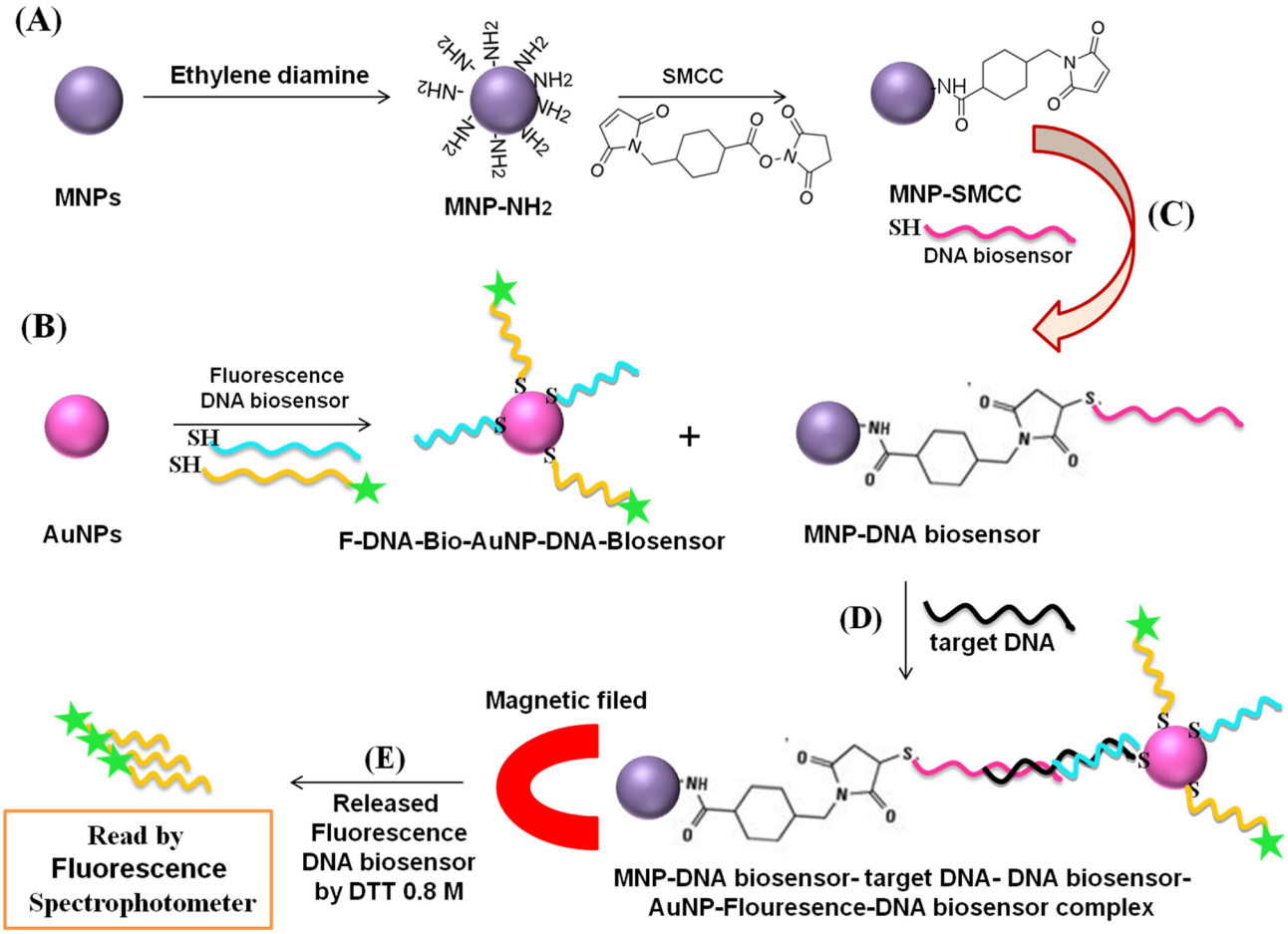

Fig. 1. Schematic of the designed Nano-biosensor: (A, C) synthesis and functionalization of MNPs; (B) Functionalization of AuNPs; (D) Formation of MNP-DNA probe$_3$-target DNA-DNA probe$_1$-AuNPs-Fluorescence DNA probe$_2$; (E) Fluorescence DNA probe$_2$ separation and release.

400–4000 cm^{-1}. The N—H stretching vibration of nucleic acid bases in the region of 1500–1700 cm^{-1} was overlapped with the amine signals of MNP-NH_2. Aside from this, in the region of 3400–3600 cm^{-1}, the wide absorbing peak of the O—H and N—H band overlaps with each other. The absorbing peaks were observed at 1700, 1612, 1666, and 1495 cm^{-1} correlated with guanine, adenine, thymine, and cytosine, respectively (Fig. 2W, curve B and curve C). Bands at 1635 and 3450 cm^{-1} refer to the NH_2 bending of the free NH_2 group and N—H stretching vibration, respectively. The presence of an absorbing peak at 626 cm^{-1} is attributed to the Fe—O bond.

3.1.4. The efficiency of conjugation

The conjugated DNA probes rates on surface of AuNPs were determined by Nano-drop and fluorescence spectrophotometry. The fluorescence intensity and the DNA probes concentration before conjugation were determined. Also, the fluorescence intensity and the DNA probes concentration after conjugation were determined by fluorescence spectrophotometry and Nano-drop spectrophotometry. For achieve this purpose, first, DNA probes on surface of AuNPs-DNA biosensors complex was released then, the absorbance rate and the fluorescence intensity were analyzed using Nano-drop and fluorescence spectrophotometry (Fig. 3A).

3.2. Optimization

The hybridization of the nanoparticle- DNA probe and target-DNA is sensitive step in designing the Nano-biosensor. Consequently, the evaluation of the effective parameters on the fluorescence intensity is necessary. In the present study, the several factors such as temperature, pH of hybridization reaction, and time of hybridization were investigated that the described in following:

3.2.1. Temperature

One of an important factor affective the fluorescence intensity was temperature hybridization. In order to, the temperature of hybridizations DNA probes with target DNA in ranges 20–60 °C were investigated under optimum condition (at pH 7.4 and a hybridization time, 50 min). The results showed that the fluorescence intensity was increased with temperature enhancement. Therefore, the optimum temperature connected target-DNA with DNA probes was at 48 °C that the fluorescence intensity was more than other temperatures (Fig. 3B).

3.2.2. Time

The effect of time on the hybridization of the target DNA and the DNA probes has been shown in Fig. 3C. Temperatures of 48 °C and pH 7.4 were used for the hybridization reaction. The fluorescence intensity was increased with the passing of time. The greatest fluorescence intensity was observed at 50 min. Also, in the more than 50 min, the fluorescence intensity was fixed and didn't change (Fig. 3C).

3.2.3. pH

The optimum pH for hybridization of target DNA with DNA probes was determined. In order to, the pH different were used forms 5 up to 9. The results showed that the maximum pH for hybridization of target DNA was 7.4 (Fig. 3D).

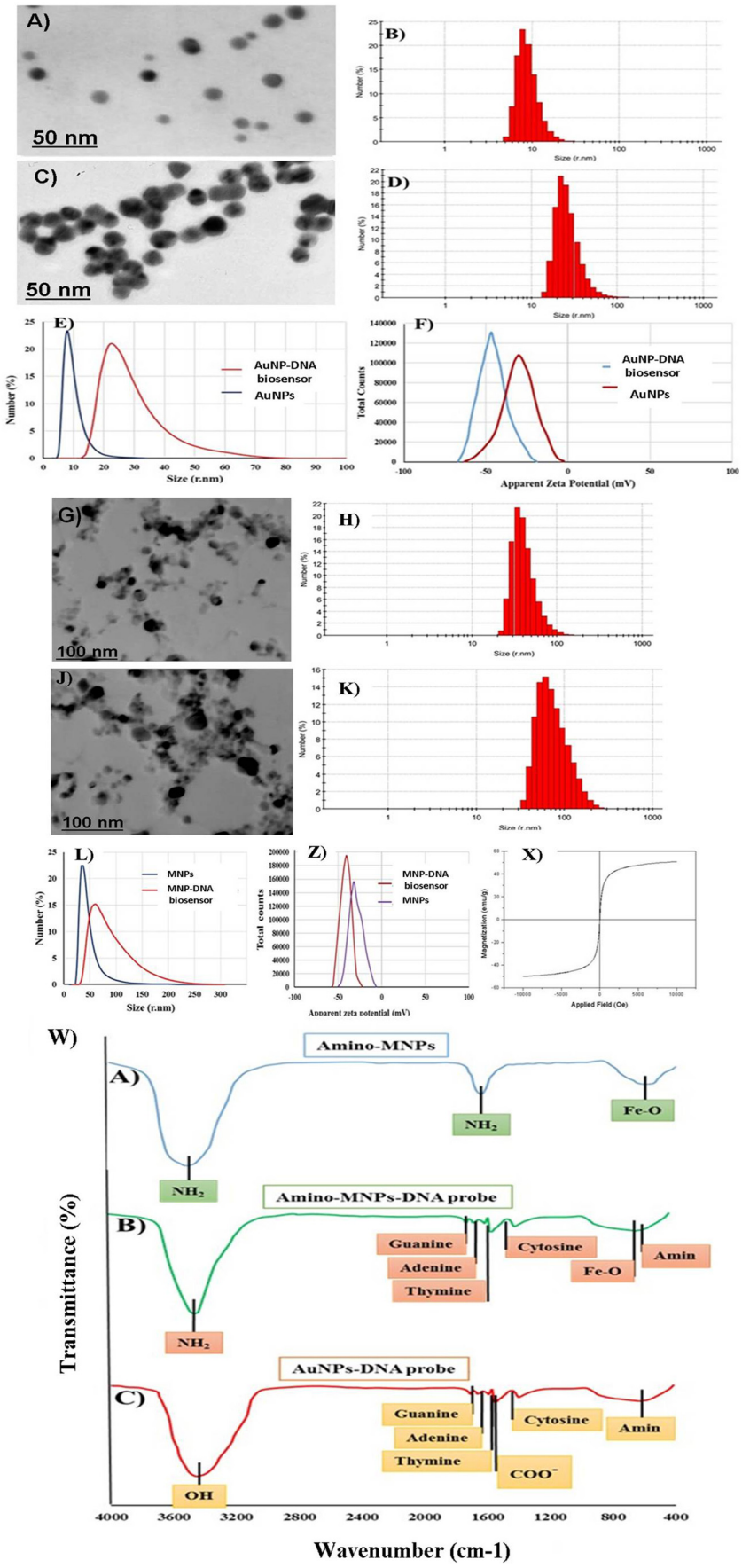

Fig. 2. Characterization of AuNPs: (A, C) TEM images of AuNPs and AuNP-DNA probes; (B, D, E, F) DLS Analysis of size and potential distribution of AuNPs and AuNP-DNA probes (G, J) TEM image of MNPs and MNP-DNA probe$_3$, (H, K, L, Z) DLS Analysis of size and potential distribution of MNPs and MNP-DNA probe$_3$; (X) Magnetization curves of MNPs TEM image, (W) FTIR spectrum of (curve, A) MNPs, (curve, B) MNP-DNA probe$_3$, (C) AuNPs-DNA probe$_3$-taget DNA.

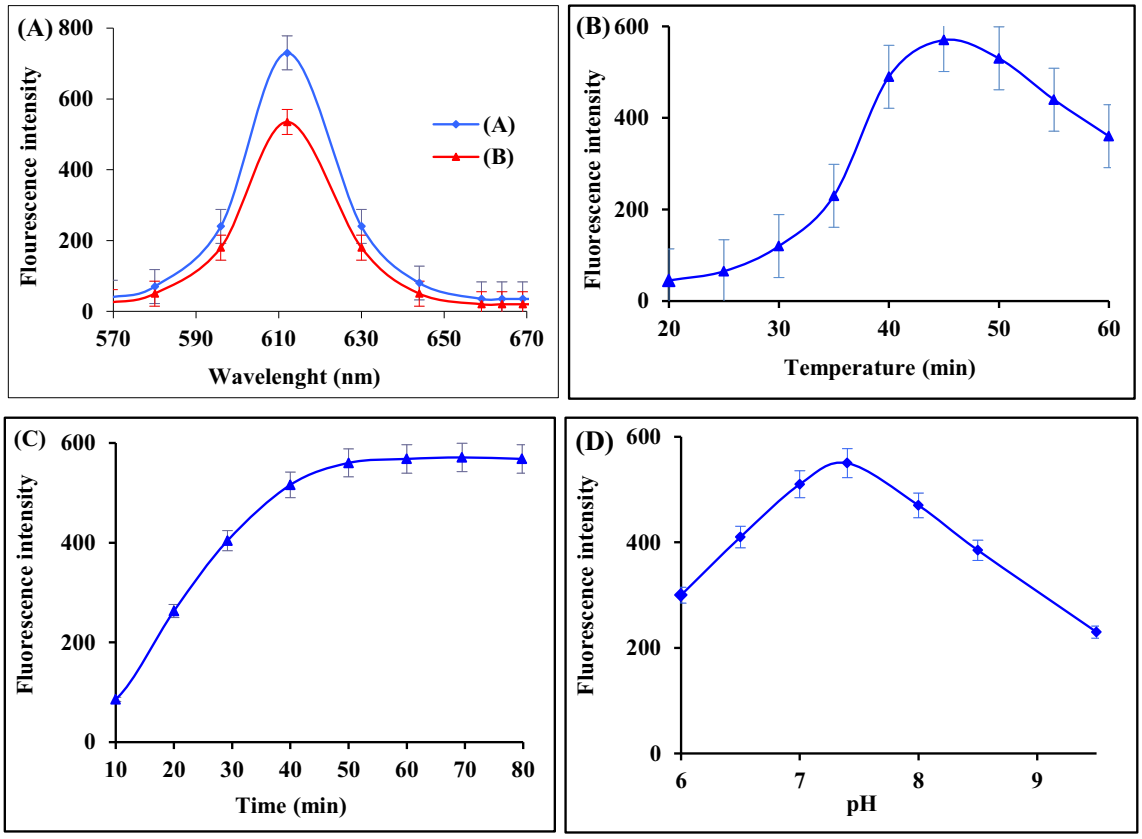

Fig. 3. Efficiency of conjugation of DNA probes on surface nanoparticels; (B) effect of temperature on hybridization; (C) effect of time on hybridization, the incubation time; (D) effect of pH on hybridization.

3.3. Sensitivity

In order to, different concentrations of extracted target DNA of bacteria (2.3×10^{1} up to 2.3×10^{9} CFU mL^{-1}) were prepared and the extracted target DNA concentrations were determined by Nano-drop spectrophotometry. Under optimum condition, the designed Nano-biosensors were added to each concentration of target DNA to formed fluorescence-DNA $probe_2$-AuNP-DNA $probe_1$-target DNA-DNA $probe_3$-SMCC-MNP complex. The complex was isolated with a magnetic field and washed three times. The fluorescence-DNA $probe_2$ complex on surface AuNPs were released by a DTT solution (0.8 M). Fluorescence intensity of the released fluorescence-DNA $probe_2$ was measured by fluorescence spectrophotometry. The results showed that with increased concentration of target DNA from 10^{2} to 10^{9} CFU mL^{-1} the fluorescence intensity were increased. Good linear related between fluorescence intensity and target DNA concentration was observed in concentration of target DNA from 10^{2} up to 10^{7} CFUmL^{-1}. The linear equation and regression were calculated that there were $Y = 1.8X + 23.4$ and R^2 0.9953 (Fig.4A, B and C). Finally the results showed that designed Nano-biosensor is capable of detecting the low concentration of the target DNA of pathogen virulence.

3.4. Limit of detection

The limit of detection (LOD) shows substantial performance characteristics in method validation. LOD is typically considered as the lowest detectable concentration of a real sample. But it is not necessarily quantified under the optimal conditions of the test. The linear relationship between fluorescence intensity and target-DNA concentration from 2.3×10^{2} up to 2.3×10^{7} were observed. The linear equation and regression were $Y = 1.8X + 23.4$ and R^2 0.9953. Therefore, the LOD was determined using the equation of $3S_a/b$, where S_a is the standard deviation of blank measurements ($n = 8$) and b is the slope of the calibration curve. Under optimal condition, the LOD was evaluated for target DNA that was 2.1 ng mL^{-1} or 90 CFU mL with correlation coefficients of $R^2_{concentration} = 0.995$. LOD of the designed Nano-biosensor was very similar with bio-barcode fluorescence sensors of Amini et al., Narmani et al. and Zhang et al. (Table 1). [21,31,34, 36, 41,43,44–47].

3.5. Specificity

The specificity of the designed fluorescent DNA biosensor for *Shigella* spp. detection was determined by the target DNA of different types of pathogens as positive and negative controls. In the present study, the targets DNA of four *Shigella spp*, *S. aureus*, *E. coli*, *V. cholera* and *P. aeruginosa* were used. Under optimum condition, Fluorescence DNA $probe_2$-AuNP-DNA $probe_1$-target DNA-DNA $probe_3$-SMCC-MNP complex were formed and released fluorescence-DNA $probe_2$. The fluorescence-DNA $probe_2$ were isolated of perception (MNPs) by a magnetic field. The fluorescence intensity of the released fluorescence-DNA $probe_2$ was measured for each sample. The results were showed in Fig. 5 that the fluorescence intensity in positive controls was more than the other pathogens as negative controls (Fig. 5, column A to D). In the negative controls (*S. aureus*, *E. coli*, *V. cholera* and *P. aeruginosa*) were not observed fluorescence intensity (Fig. 5, column E to H). The results showed that the designed Nano-biosensor was completely specificities and selectivity for detection of *Shigella spp* (*Shigella dysenteriac* (Fig. 5, column A), *Shigella flexneri* (Fig. 5, column B), *Shigella boydii* (Fig. 5, column C), *Shigella sonnei* (Fig. 5, column D). In the present study, the used target DNA concentrations in negative and positive controls were 150 ng mL^{-1} or 2.3×10^{6} CFU mL^{-1}.

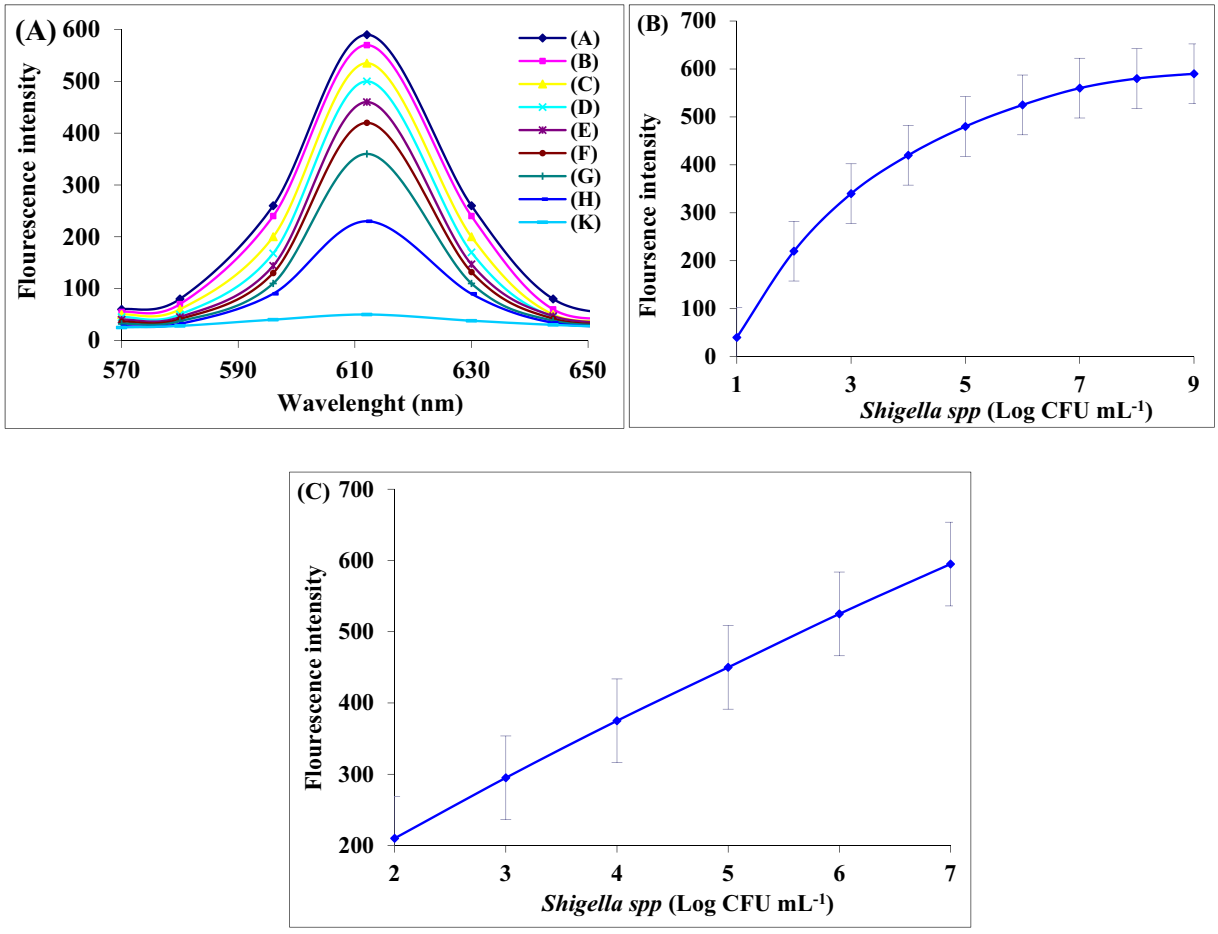

Fig. 4. (A) Fluorescence intensity in different concentrations of 2.3×10^{1} up to 2.3×10^{9} CFU mL^{-1} from K to A (target DNA), (B) linear relationships between flourescence intensity and concentrations of *Shigella spp* from 2.3×10^{1} up to 2.3×10^{9} CFU mL^{-1} (target DNA), (C) standard curve between fluorescence intensity and concentrations of *Shigella spp* from 10^{2} up to 10^{7} CFU mL^{-1} (target DNA).

Table 1
Compare of detection limit of *Shigella spp* using different methods.

Method	Detection limit	References
Silica nanoparticle-probe assay	682 CFU mL^{-1}	[45]
Colorimetric assay	3.2×10^{2} CFU mL^{-1}	[37]
Loop-mediated isothermal amplification (LAMP)	6.4×10^{3} CFU mL^{-1}	[45]
Quantum dots	1×10^{2} CFU mL^{-1}	[43]
enzyme-linked immunosorbent assay (ELISA)	1×10^{4} CFU mL^{-1}	[45]
PCR assay	1.6×10^{3} CFUmL^{-1}	[8]
Electrochemical assay	1×10^{2} CFU mL^{-1}	[2]
Fluorescence DNA biosensors assay	90 CFU mL^{-1}	Our method

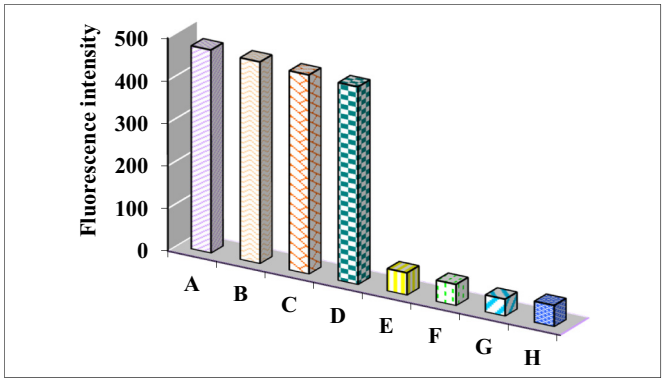

Fig. 5. Specificity of designed Nano-biosensor, (column A) the fluorescence intensity of *Shigella dysenteriac* (column A), *Shigella flexneri* (column B), *Shigella boydii* (column C), *Shigella sonnei* (column D) as positive controls, *P. aeruginosa* (column E), *S. aureus* (column F), *E. coli* (column G) and *V. cholera* (column H) as negative controls, (the target DNA concentration: 150 ng mL^{-1}).

3.6. Real samples

The accuracy of the fluorescence-DNA biosensor assay, the recovery of target DNA was measured. The results were presented in Table 2. The results confirmed the recoveries of target DNA were obtained in clinical samples in the range of 97.5–104.5%. Also, each sample was replicated three times. The genomic DNA concentrations were showed in Table 2. These results indicated that the nanomaterial's system was exacted and repeatable for detection of *Shigella spp* in clinical samples.

4. Conclusion

In the present study, a pair Nano-biosensor based on Iron and gold nanoparticles were designed for the detection of multi-*Spa* genes in *Shigella spp* for first time. The DNA probes were immobilized on surface of AuNPs and MNPs. The fluorescence DNA $probe_1$ on the surface of AuNPs was as signal reporter. Other DNA probes on the surface of AuNPs and MNPs were as connector and separator of target DNA. The fluorescence DNA $probe_2$-AuNP-DNA $probe_1$ and DNA $probe_3$-MNPs were added to target DNA to formed fluorescence DNA $probe_1$-AuNP-DNA $probe_1$-target DNA-DNA $probe_3$-MNPs complex. The complex was separated with a magnetic field and fluorescence DNA $probe_2$ was

Table 2
The recovery and RSD value of detecting *Shigella spp*.

Analyses	Added target DNA ($ng\,mL^{-1}$)	Found ($ng\,mL^{-1}$)	Recovery (%)	RSD (%)
1	10	10.18	101.8	4.03
2	20	19.5	97.5	6.0
3	30	31.0	103.3	6.3
4	40	39.8	98.0	4.0
5	50	49.7	98.5	5.8
6	60	61.96	104.5	7.2

released on surface of AuNPs. Fluorescence intensity, the released fluorescence DNA probe$_2$ was measured by fluorescence spectrophotometry. The sensitivity and specificity of designed Nan-biosensor were determined. The results showed that the linear relationship between target DNA concentration and fluorescence intensity were in concentration of 2.3×10^{2} up to 2.3×10^{7} CFU mL^{-1}. The LOD was determined 2.1 ng mL or 90 CFU mL^{-1}. The size and potential of the AuNPs after conjugation was changed form 15 nm, −32.2 mV and 23–28 nm, −25 mV to 18 nm, −18 mV and 43 nm, −15 mV, respectively. The specificity and sensitivity of the designed fluorescent DNA biosensor were determined which were good enough for the precise detection of *Spa* gene in four *Shigella* spp. at low concentrations bacteria (CFU mL^{-1}). Therefore, the current method will provide a highly sensitive detection method for high-risk pathogens in the future.

Declaration of competing interest

The authors report no conflicts of interest in this work.

References

[1] M. Getamesay, B. Getenet, Z. Ahmed, Prevalence of shigella, salmonella and cmpylobacter species and their susceptibility patters among under five children with diarrhea in hawassa town, south Ethiopia, Ethiop. J. Health Sci. 24 (2014) 101–108.

[2] J. Luo, J. Wang, A.S. Mathew, et al., Ultrasensitive detection of Shigella species in blood and stool, Anal. Chem. 88 (2016) 2010–2014.

[3] H. Zhang, Y. Zhang, Y. Lin, et al., Ultrasensitive detection and rapid identification of multiple foodborne pathogens with the naked eyes, Biosens. Bioelectron. 71 (2015) 186–193.

[4] N. Bhardwaj, S.K. Bhardwaj, M.K. Nayak, et al., Fluorescent nanobiosensors for the targeted detection of foodborne bacteria, TrAC Trends Anal. Chem. 97 (2017) 120–135.

[5] J.W.F. Law, N.S. Ab Mutalib, K.G. Chan, et al., Rapid methods for the detection of foodborne bacterial pathogens: principles, applications, advantages and limitations, Front. Microbiol. 5 (2015) 770.

[6] X. Zhao, C.-W. Lin, J. Wang, et al., Advances in rapid detection methods for foodborne pathogens, J. Microbiol. Biotechnol. 24 (2014) 297–312.

[7] B. Amini, et al., Cloning of catalytic domain of exotoxin A from *Pseudomonas aeruginosa*, J. Zanjan Univ. Med. Sci. Health Serv. 71 (2010) 24–33.

[8] R. Binet, D.M. Deer, S.J. Uhlfelder, Rapid detection of *Shigella* and enteroinvasive Escherichia coli in produce enrichments by a conventional multiplex PCR assay, Food Microbiol. 40 (2014) 48–54.

[9] M. Koziel, D. Corcoran, I. Ocallaghan, et al., Validation of the EntericBio panel II multiplex polymerase chain reaction system for detection of campylobacter spp., Salmonella spp, Shigella spp, and verotoxigenic E. coli for use in a clinical diagnostic setting, Diagn. Microbiol. Infect. Dis. 75 (2013) 46–49.

[10] S.C. Ojha, C. Yean, A. Ismail, et al., A pentaplex PCR assay for the detection and differentiation of Shigella species, Biomed. Res. Int. (2013) 1–9, https://doi.org/10.1155/2013/412370.

[11] F. Barletta, E. Mercado, A. Lluque, et al., Multiplex real-time PCR for detection of *Campylobacter*, *Salmonella*, and *Shigella*, J. Clin. Microbiol. 51 (9) (2013) 2822–2829.

[12] R. Shahbazi, M. Salouti, B. Amini, et al., Highly selective and sensitive detection of Staphylococcus aureus with gold nanoparticle-based core-shell nano biosensor, Mol. Cell. Probes 41 (2018) 8–13.

[13] K. Ma, Y. Deng, Y. Bai, et al., Rapid and simultaneous detection of *Salmonella*, *Shigella*, and *Staphylococcus aureus* in fresh pork using a multiplex real-time PCR assay based on immunomagnetic separation, Food Control 42 (2014) 87–93.

[14] D. Wiemer, U. Loderstaedt, H. Von Wulffen, et al., Real-time multiplex PCR for simultaneous detection of *Campylobacter jejuni*, *Salmonella*, *Shigella* and *Yersinia* species in fecal samples, Int. J. Med. Microbiol. 301 (2011) 577–584.

[15] K.W. Soli, M. Kas, T. Maure, et al., Evaluation of colorimetric detection methods for *Shigella*, *Salmonella*, and *Vibrio cholerae* by loop-mediated isothermal amplification, Diagn. Microbiol. Infect. Dis. 77 (2013) 321–323.

[16] W. Mokhtari, S. Nsaibia, A. Gharbi, et al., Real-time PCR using SYBR green for the detection of *Shigella spp*. in food and stool samples, Mol. Cell. Probes 27 (2013) 53–59.

[17] A. Singh, S. Poshtiban, S. Evoy, Recent advances in bacteriophage based biosensors for food-borne pathogen detection, Sensors 13 (2013) 1763–1786.

[18] R. Xiao, Z. Rong, F. Long, et al., Portable evanescent wave fiber biosensor for highly sensitive detection of *Shigella*, Spectrochim. Acta A Mol. Biomol. Spectrosc. 132 (2014) 1–5.

[19] Y. Lv, S. Chen, Y. Shen, et al., Competitive multiple-mechanism-driven electrochemiluminescent detection of 8-hydroxy-2′-deoxyguanosine, J. Am. Chem. Soc. 140 (2018) 2801–2806.

[20] Y. Shen, Y. Zhang, Q. Zhang, et al., Immobilization of ionic liquid with polyelectrolyte as carrie, Chem. Commun. 33 (2005) 4193–4195.

[21] B. Amini, M. Kamali, M. Salouti, et al., Fluorescence bio-barcode DNA assay based on gold and magnetic nanoparticles for detection of exotoxin A gene sequence, Biosens. Bioelectron. 92 (2017) 679–686.

[22] K. Kant, M.A. Shahbazi, V.P. Dave, et al., Microfluidic devices for sample preparation and rapid detection of foodborne pathogens, Biotechnol. Adv. 36 (2018) 1003–1024.

[23] J. Ji, J. Wen, Y. Shen, et al., Simultaneous noncovalent modification and exfoliation of 2D carbon nitride for enhanced electrochemiluminescent biosensing, J. Am. Chem. Soc. 139 (2017) 11698–11701.

[24] Y. Lv, Z. Zhou, Y. Shen, et al., Coupled fluorometer-potentiostat system and metal-free monochromatic luminophores for high-resolution wavelength resolved electrochemiluminescent multiplex bioassay, ACS Sens 3 (2018) 1362–1369.

[25] A. Amini, M. Kamali, B. Amini, et al., Enhanced antibacterial activity of imipenem immobilized on surface of spherical and rod gold nanoparticles, J. Phys. D. Appl. Phys. 5 (2019), https://doi.org/10.1088/1361-6463/aaef4d in press.

[26] C. Zhang, P. Du, Z. Jiang, et al., A simple and sensitive competitive bio-barcode immunoassay for triazophos based on multi-modified gold nanoparticles and fluorescent signal amplification, Anal. Chim. Acta 999 (2018) 123–131.

[27] H.B. Wang, H.Y. Bai, G.L. Dong, et al., DNA-templated Au nanoclusters coupled with proximity-dependent hybridization and guaninerich DNA induced quenching: a sensitive fluorescent biosensing platform for DNA detection, Nanoscale Advances 1 (2019) 1482–1488.

[28] E. Alveroglu, H. Sozeri, A. Baykal, et al., Fluorescence and magnetic properties of hydrogels containing Fe3O4 nanoparticles, J. Mol. Struct. 1037 (2013) 361–366.

[29] K. Rajar, B. Karakus, K. Koc, et al., One pot synthesis and characterization of Fe3O4 nanorod-PNIPA nanogel composite for protein adsorption, Mater. Sci. Eng. C 68 (2016) 59–64.

[30] K. Koc, E. Alveroglu, Adsorption and desorption studies of lysozyme by Fe3O4–polymer nanocomposite via fluorescence spectroscopy, J. Mol. Struct. 1089 (2015) 66–72.

[31] A. Amini, M. Kamali, B. Amini, et al., Bio-barcode technology for detection of Staphylococcus aureus protein A based on gold and iron nanoparticles, Int. J. Biol. Macromol. 124 (2019) 1256–1263.

[32] H.B. Wang, Y. Li, Y. Chen, et al., Determination of the activity of alkaline phosphatase by using nanoclusters composed of flower-like cobalt oxyhydroxide and copper nanoclusters as fluorescent probes, Microchim. Acta 185 (2) (2018) 102.

[33] H.B. Wang, H.D. Zhang, Y. Chen, et al., A fluorescent biosensor for protein detection based on poly (thymine)- templated copper nanoparticles and terminal protection of small molecule-linked DNA, Biosens. Bioelectron. 74 (2015) 581–586.

[34] A. Narmani, M. Kamali, B. Amini, et al., Highly sensitive and accurate detection of Vibrio cholera O1 OmpW gene by fluorescence DNA biosensor based on gold and magnetic nanoparticles, Process Biochem. 65 (2018) 46–54.

[35] N. Elahi, M. Kamali, M.H. Baghersad, Recent biomedical applications of gold nanoparticles: a review, Talanta 184 (2018) 537–556.

[36] Y. Cherradi, A. Hachani, A. Allaoui, Spa13 of *Shigella flexneri* has a dual role: chaperone escort and export gate-activator switch of the type III secretion system, Microbiology 160 (2014) 130–141.

[37] B. Amini, M. Kamali, M. Salouti, P. Yaghmaei, Spectrophotometric, colorimetric and visually detection of *Pseudomonas aeruginosa* ETA gene based gold nanoparticles DNA probe and endonuclease enzyme, Spectrochim. Acta A 199 (2018) 421–429.

[38] M. Song, D.J. Sukovich, L. Ciccarelli, et al., Control of type III protein secretion using a minimal genetic system, Nat. Commun. 8 (2017) 14737, , https://doi.org/10.1038/ncomms14737.

[39] Z. Chen, C. Zhang, T. Zhou, et al., Gold nanoparticle based colorimetric probe for dopamine detection based on the interaction between dopamine and melamine, Microchim. Acta 182 (2015) 1003–1008.

[40] L. Shi, E. Buhler, F. Boué, et al., How does the size of gold nanoparticles depend on citrate to gold ratio in Turkevich synthesis, final answer to a debated question, J. Colloid Interface Sci. 492 (2017) 191–198.

[41] N. Songvorawit, K. Tuitemwong, P. Tuitemwong, Single step synthesis of amino-functionalized magnetic nanoparticles with polyol technique at low temperature, ISRN Nanotechnology (2011) 1–6, https://doi.org/10.5402/2011/483129.

[42] A. Narmani, M. Kamali, B. Amini, et al., Targeting delivery of oxaliplatin with smart PEG-modified PAMAM G4 to colorectal cell line in vitro studies, Process Biochem. 69 (2018) 178–187.

[43] D. Zhang, M.C. Huarng, E.C. Alocilja, A multiplex nanoparticle-based bio-barcoded DNA sensor for the simultaneous detection of multiple pathogens, Biosens. Bioelectron. 26 (2010) 1736–1742.

[44] N. Elahi, M. Kamali, M.H. Baghersad, Precise, direct, and rapid detection of *Shigella Spa* gene by a novel unmodified AuNPs-based optical genosensing system, J. Microbiol. Methods 162 (2019) 42–49.

[45] A. Narmani, M. Rezvani, B. Farhood, et al., Folic acid functionalized nanoparticles as pharmaceutical carriers in drug delivery systems, Drug Dev. Res. 80 (2019) 404–424.
[46] A. Liu, K. Yin, L. Mi, et al., A novel photoelectrochemical immunosensor by integration of nanobody and ZnO nanorods for sensitive detection of nucleoside diphosphatase kinase-a, Anal. Chim. Acta 973 (2017) 82–90.
[47] Y. Liu, M. Wei, L. Zhang, et al., Chiroplasmonic assemblies of gold nanoparticles for ultrasensitive detection of 8-hydroxy-2′-deoxyguanosine in human serum sample, Anal. Chem. 88 (2016) 6509–6514.